Applied Chemistry Today **19(73)** (2024) 253-268

Semnan University

Applied Chemistry Today

Journal homepage: https://chemistry.semnan.ac.ir/

ISSN: 2981-2437

Research Article

New Metal Complexes Incorporating Schiff Base Ligand Based on Hydrazide Moiety: Synthesis, Spectral Characterization, Electrochemical behavior, and Molecular Docking

Sakineh Parvarinezhad, Mehdi Salehi*

Department of Chemistry, Faculty of Science, Semnan University, Semnan, Iran

PAPER INFO

Article history:
Received: 03/Nov/2024
Revised: 01/Dec/2024
Accepted: 06/Dec/2024

Keywords:
4-hydroxybenzohydrazide;
Schiff base;
Cu(II) complex;
Electrochemical behavior (CV);
docking study.

ABSTRACT

In the last four years, the coronavirus-infectious disease and the preparation of compounds with suitable biological properties as medicine to prevent and deal with these diseases have attracted the attention of the medical community and the World Health Organization (WHO). Among the chemical compounds that have shown appropriate biological and medicinal properties against various diseases, including cancer, hepatitis, and corona, are compounds of hydrazide derivatives. In the present work, two new copper complexes were synthesized starting from a 4-hydroxybenzohydrazide Schiff base ligand with benzaldehyde derivatives. Elemental analysis, spectral data (FT-IR and UV-Vis spectroscopic techniques), and cyclic voltammetry (CV) were used to confirm their structures. The inhibitory effect of the studied copper complexes against two coronaviruses, proteins with codes 6Y2F and 6M0J, was evaluated using the molecular docking method. The results indicate that these compounds exhibit better performance, with a total system energy of approximately -81.34 kcal/mol for structure (**1**) (associated with protein 6Y2F) and a total energy of -135.68 kcal/mol for structure (**2**) (related to the coronavirus 6M0J). These values are comparable with those reported for similar structures, further supporting the potential efficacy of these compounds. As such, it is suggested that these compounds could serve as promising candidates for addressing coronavirus infections. By assessing the inhibitory properties of copper complexes through molecular docking analyses, these findings offer valuable insights into the potential utility of these compounds in combating coronaviruses.

DOI: https://doi.org/10.22075/chem.2024.35796.2321

* **.Corresponding author:** Professor of Inorganic Chemistry. *Email address: msalehi@semnan.ac.ir*

How to cite this article: Parvarinezhad, S. & Salehi, M. (2024). New Metal Complexes Incorporating Schiff Base Ligand Based on Hydrazide Moiety: Synthesis, Spectral Characterization, Electrochemical behavior, and Molecular Docking. *Applied Chemistry Today*, **19(73)**, 253-268. (in Persian)

1. Introduction

Schiff base complexes have been used in many fields due to their structural diversity [1-4]. Hydrazones, synthesized from aldehydes and hydrazines, act as essential precursors for coordination with transition metals, leading to the formation of new complexes with diverse biological properties [5]. Notably, hydrazone derivatives with ONO and NNO donor atoms have emerged as important components in coordination chemistry [6, 7]. These compounds have shown a wide range of physiological, and biological activities, including anticancer, antibacterial, antioxidant, antifungal, antituberculosis, and anti-inflammatory properties [8-13]. The synthesis of copper, cobalt and nickel Schiff base complexes derived from hydrazones has been the subject of researchers' attention [14-19]. Current studies emphasize the importance of designing and synthesizing metal-based agents for cancer chemotherapy in the realm of inorganic medicinal chemistry. Recent literature reviews have highlighted the anticancer potential of metal complexes derived from hydrazones, particularly those involving cobalt, nickel, and copper complexes. Among complexes, copper complex plays a prominent role in biological processes and chemical development of drugs. In addition, these complexes are of interest due to their biological properties such as redox reactions, metabolic pathways, and cell growth. Their physicochemical properties, including electrical conductivity and magnetism, are widely used for the synthesis of products such as dihydrotestosterone, cytotoxic activity, antimicrobial or analgesic properties, and biocompatibility similar to ampicillin and streptomycin [20, 21]. In addition, research has been conducted on the antibacterial properties of hydrazone derivatives against Gram-positive and Gram-negative bacteria [22-28]. In a present study, two Schiff base metal complexes derived from 4-hydroxybenzohydrazide, with benzaldehyde ligands were prepared and characterized according to established methods [29-30]. Based on previous findings [31, 32], the 4-hydroxybenzohydrazide-derived ligand was identified as a tridentate ligand, which led to the adoption of a 5-coordinated square pyramidal polymeric structure by the copper complexes (Scheme 1). The synthesized copper complexes were further characterized through infrared spectroscopy, electron transmission, and elemental analysis methods. After that, the inhibitory effects of these copper complexes against two coronaviruses were evaluated using molecular docking techniques. This study aims to compare the biological activities of the synthesized compounds, providing valuable insights into their potential medicinal applications. Research on Schiff base metal complexes derived from hydrazones emphasizes the versatility and multifaceted biological activities of these compounds and provides a foundation for further exploration in drug development and therapeutic interventions against various diseases including coronaviruses.

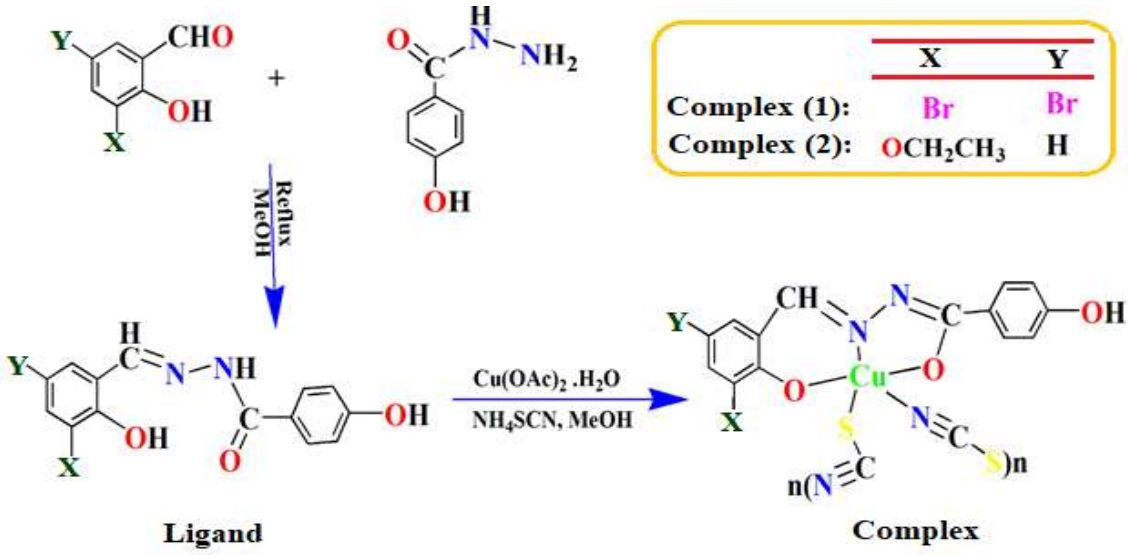

Scheme 1. Synthetic procedure for the preparation of the Cu(II) complexes hydrazide-based Schiff bases.

2. Experimental method

2.1. Chemicals and devices

All chemicals and solvents used in this research were purchased with synthetic grade from Merck and Aldrich. Infrared (IR) spectra were reported by the Shimadzu 8400S transform infrared spectrometer using potassium bromide tablets. Electron transition spectra (UV-Vis) were recorded in dimethyl sulfoxide solvent using a Shimadzu UV-1650 PC spectrophotometer device. Elemental analyses were done on an Elmental Vario CHNSO and PerkiElmerer device. Electrochemical behavior (CV) was performed on a Metrohm 757 VA Computrace instrument at room temperature in dimethyl sulfoxide solution.

2.2. Synthesis method of ligands derived from 4-hydroxybenzohydrazide

The Schiff base ligands **HL^1-HL^2** were synthesized from the condensation of 3,5-dibromo2-hydroxybenzaldehyde, 2-hydroxy3-ethoxybenzaldehyde with 4-hydroxybenzohydrazide according to the Schiff base methods mentioned in the sources [32-34] and was used in the synthesis of complexes.

2.2.3. Synthesis of Cu (II)-hydrazide complexes

The amount of 5 mmol (0.2 g) of the ligand was dissolved in 10 ml of methanol. Then, 5 mmol (0.1 g) of copper (II) acetate was dissolved in methanol solvent separately and added drop by drop to the ligand solution and the color of the solution changed from yellow to green. After 30 minutes, the amount of 5 mmol (0.38 g) of ammonium thiocyanide was added to the solution and it was placed under reflux conditions for 10 hours at room temperature. After finishing the work, the final solution was filtered and the contents of this synthesis were put to rest in laboratory conditions for the crystallization process. After 13 days, after the slow evaporation of the solvent, a green crystal was observed. The fine crystal from this synthesis was filtered from the solution by a vacuum pump device and a Buchner funnel. The structure of this complex was identified using spectroscopic analysis and elemental analysis and is presented in section 3 along with the electrochemical results.

Complex (1):

Green crystals. Yield: 75%. Mol. Wt: 546.68 g/mol. Anal. Calc. for $C_{16}H_9Br_2CuN_3O_3S$: C, 35.15; H, 1.66; N:7.69 %. Found: C, 35.04; H; 1.28; N, 7.38%. FT-IR: (KBr, cm^{-1}): 3416(υ_{O-H}), 3080 (υ_{N-H}), 2953, 2923(υ_{C-H}), 2111(υ_{S-CN}), 1608, 1587($\upsilon_{C=N}$), 1382, 1361(υ_{C-O}), 642-759 (υ_{M-O}), 547-622(υ_{M-N}). UV–Vis: λ_{max} (nm) (ε, M^{-1} cm^{-1}) (DMSO): 286(110000), 312(26000), 320(32000), 330(35000), 384(31000), 392(31000), 609(690).

Complex (2):

Green crystals. Yield: 61%. Mol. Wt: 432.94 g/mol. Anal. Calc. for $C_{18}H_{15}CuN_3O_4S$: C, 49.94; H, 3.49; N:9.71 %. Found: C, 49.54; H; 3.33; N, 9.34%. FT-IR: (KBr, cm^{-1}): 3226(υ_{O-H}), 3064 (υ_{N-H}), 2977, 2927(υ_{C-H}), 2065(υ_{S-CN}), 1604, 1560($\upsilon_{C=N}$), 1388, 1375(υ_{C-O}), 688-759 (υ_{M-O}), 640 (υ_{M-N}). UV–Vis: λ_{max} (nm) (ε, M^{-1} cm^{-1}) (DMSO): 280(4800), 360(14600), 398(13400), 421(8700), 605(820).

2.2.4. Electrochemical Studies Using Cyclic Voltammetry

In the electrochemical studies conducted using cyclic voltammetry (CV), the oxidation and reduction potential values, as well as the electrochemical behavior of the synthesized copper complexes, were examined. The experimental setup required silver wire reference electrodes, platinum auxiliary electrodes, and glassy carbon work electrodes for the electrochemical analysis. Additionally, the analysis necessitated the use of an electrolyte solution; thus, a 10^{-1} M concentration of tetrabutylammonium hexafluorophosphate salt in dimethyl sulfoxide solution was employed to prepare the electrolyte solution. The cyclic voltammogram process was conducted at a temperature of 25°C under argon gas conditions to eliminate oxygen from the reaction medium. A scanning speed of 100 mV/s was employed during the cyclic voltammetry analysis. Following each scan, the working electrode was polished with alumina powder to eliminate any potential contamination. Notably, all the potentials of the oxidation and reduction regions were calibrated using ferrocene as an internal standard ($E_{1/2}$ = 0.42 V) for accurate measurements [35, 36]. The electrochemical behavior information, including oxidation and reduction values, along with the cyclic voltammogram diagrams of the prepared complexes, will be detailed in the subsequent section of this study, offering valuable insights into the redox properties and reactivity of the synthesized copper complexes in different electrochemical environments.

2.2.5. Molecular docking

The protein-ligand interaction between the copper polymer complexes and the target proteins (proteins with the codes 6Y2F and 6M0J in the case of the coronavirus (https://www.rcsb.org/structure/6Y2F and 6M0J)) has been determined using the molecular docking method and the Molegro Virtual Docker & Molegro Molecular Viewer software. It should be mentioned that first the structure of copper complexes (**1** and **2**) was optimized using the B3LYP/6-311+G method in Gaussian09 software and then, the optimized structures were used as pdb files for docking simulations. Heteroatoms, ligands, and water molecules in the studied biological structures were removed with the help of Discovery Studio software. Also, 2D and 3D shapes were drawn using Discovery Studio software [37-40].

3. Results and discussion

3.1. Synthesis

In this study, two copper complexes of 4-hydroxybenzohydrazide derivatives were prepared and identified. Identification of these complexes was done using infrared spectrum (FT-IR), electron transfer (UV-Vis), electrochemical behavior (CV) and elemental analysis. The bioinformatics analysis presented in this study is based on the molecular docking method, and the results show that copper polymer complexes have very good inhibitory activity against the receptors of two coronaviruses 6Y2F and 6M0J. So the total energies calculated for both complexes have small and negative values, which show that the complex has interacted well with amino acids and the amino acids are placed in the active and effective position.

3.2. FT-IR spectra of the ligands ($HL^{1,2}$) and complexes (1 and 2)

FT-IR spectra provide valuable information about ligand coordination with metal ion. **Figs. (1-4)** show the FT-IR spectrum of ligands (**$HL^{1,2}$**) and copper (II) complexes (**1** and **2**), respectively. In the spectrum of the **$HL^{1,2}$** ligands, bands have appeared

in the regions of 1647 and 1604 cm^{-1} (for **HL[1]**) and1647 and 1598 cm^{-1} (for **HL[2]**) which belong to the $\upsilon_{(C = O)}$ and $\upsilon_{(C = N)}$ stretching vibrations, respectively. The $\upsilon_{(C = N)}$ regions in the spectrum of the complexes (**1** and **2**) have been shifted to higher energies and to the wave numbers of 1587 and 1608 cm^{-1} (for complex (**1**)) and 1560 , 1604 cm^{-1} (for complex (**2**)), these results show that the ligand is coordinated with the metal ion through the nitrogen atom of the azomethine group. Also, the deprotonation of the phenolic group and the absence of O-H stretching bands in the region of 3461 and 3469 cm^{-1} indicate the formation of the complexes. In addition, the M-O and M-N stretching bands in the complexes respectively have a lower wavenumber in the range of 642-759 and 622-1547 cm^{-1} (for complex (**1**)) as well as, 688-759 and 640 cm^{-1} (for complex (**2**)) appeared. The strong band at 2111cm^{-1} (for complex (**1**)) and 2065 cm^{-1} (for complex (**2**)) is attributed to the presence of the SCN group in the complex. Also, in the free ligand, the phenolic C-O stretching vibration bands are assigned in the regions of 1301 and 1350 cm^{-1} (for **HL[1, 2]**), which in the complex is shifted to a higher wave number of 1361-1382 cm^{-1} (for complex (**1**)) as well as, 1375-1388 cm^{-1} (for complex (**2**)) which also confirms that the coordination phenolic oxygen is the ligand to copper ion [31, 41-45]. The C-H stretching vibrational mode is observed in the region of 2700-3200 cm^{-1}.

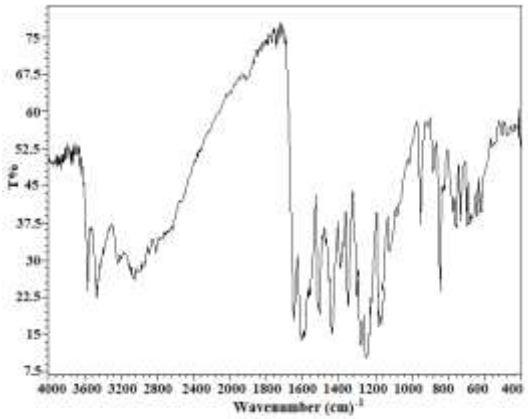

Figure. 1 Displays the FT-IR spectrum of the (**HL[1]**).

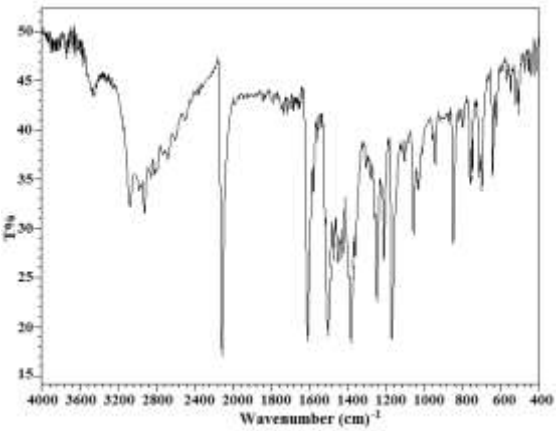

Figure. 2 Displays the FT-IR spectrum of the Complex (**1**).

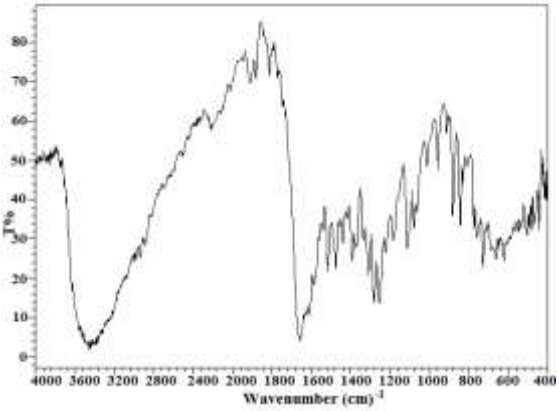

Figure. 3 Displays the FT-IR spectrum of the (**HL[2]**).

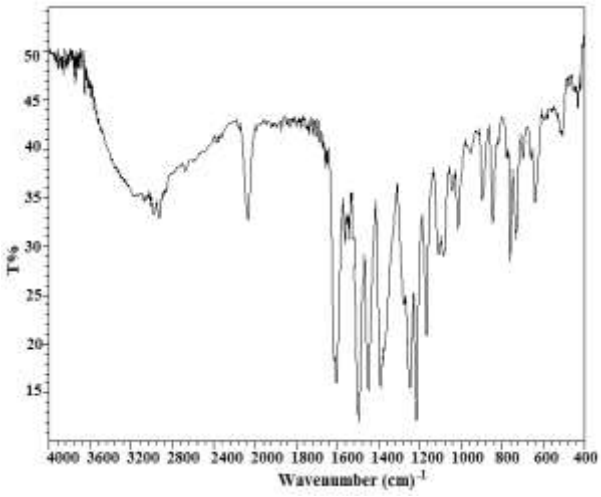

Figure. 4 Displays the FT-IR spectrum of the Complex (**2**).

3.3. UV-Vis Spectra Analysis of (HL[1, 2]) and complexes (1and 2)

The UV-Vis spectra of the **HL[1, 2]** ligands, and complex (**1** and **2**) were analysed to gain insights into the electronic absorption properties of the compounds. The electron absorption spectra were recorded in a dimethyl sulfoxide solution with

concentrations of 10^{-5} M for the ligands and 10^{-3} M and 10^{-5} M for complex (**1** and **2**), spanning a wavelength range of 200-800 nm at room temperature (**Figs. (5-8)**). In the UV-Vis spectrum of the Schiff base ligands, distinct peaks were observed, with a strong peak detected around 240 and 248 nm (for **HL^{1}**), and 238 nm (for **HL^{2}**) attributed to the π → π * transition of the aromatic ring. The peaks at 263 and 282 nm nm (for **HL^{1}**), and 300 nm were assigned to the π → π * transition of the azomethine group. Furthermore, the peak observed at 385, 378 nm corresponds to the n → π * transition of the azomethine group, demonstrating the electronic transitions within the ligands (**HL$^{1, 2}$**) molecule, respectively. Conversely, the spectrum of electronic transitions of complexes (**1** and **2**) exhibited bands in the ultraviolet region, manifesting distinctive peaks at 320, 330, 384, and 392 nm (for complex (**1**)) and 360, 398, and 421 nm (for complex (**2**)). These peaks were linked to intra-ligand transitions of the azomethine group and MLCT (metal-to-ligand charge transfer) transitions, suggestive of complex formation. Notably, the emergence of higher wavelength bands indicated the coordination of the copper ion to the azomethine group (C = N). Additionally, a broad shoulder at 609 and 605 nm (for complex (**1**) and (for complex (**2**), respectively) was observed in the spectrum, corresponding to the d → d transitions of the copper complex, providing further insights into the electronic structure and coordination environment of the copper ion within the complexes [31, 41-45].

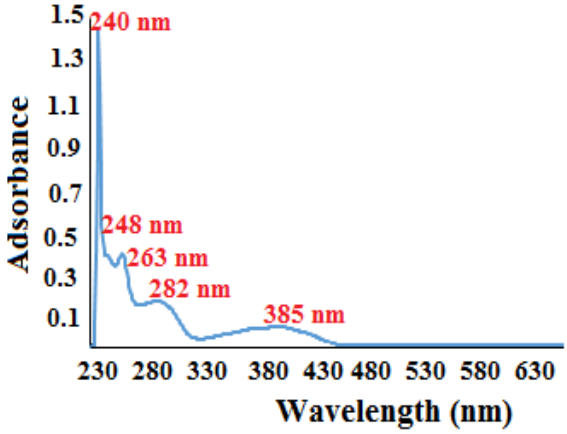

Figure. 5 Show the UV-Vis spectrum of **HL^{1}**.

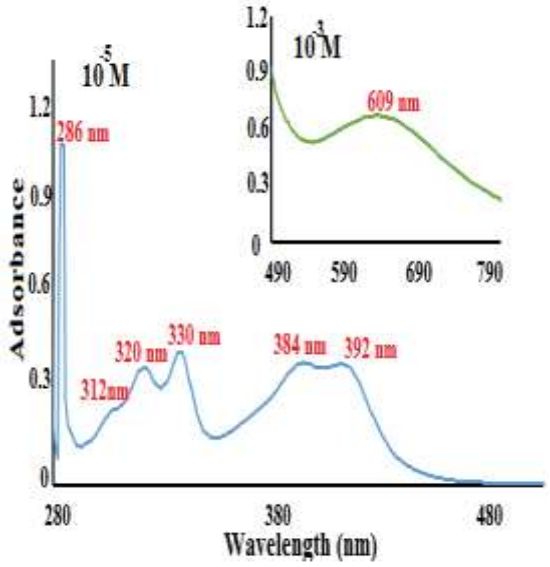

Figure. 6 Show the UV-Vis spectrum of copper complex (**1**) with a concentration of 10^{-5} mol/L and with 10^{-3}mol/L in the DMSO.

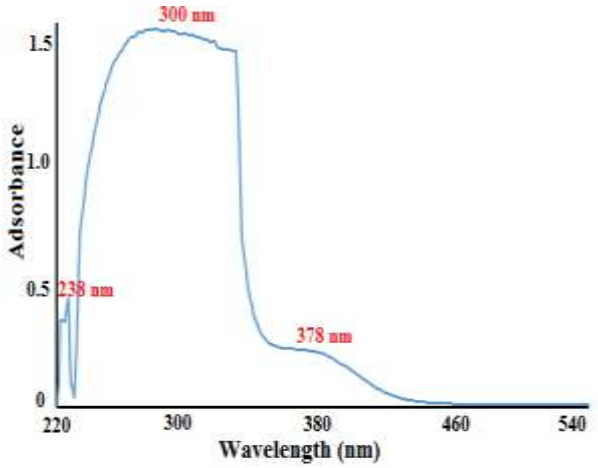

Figure. 7 Show the UV-Vis spectrum of **HL**[2].

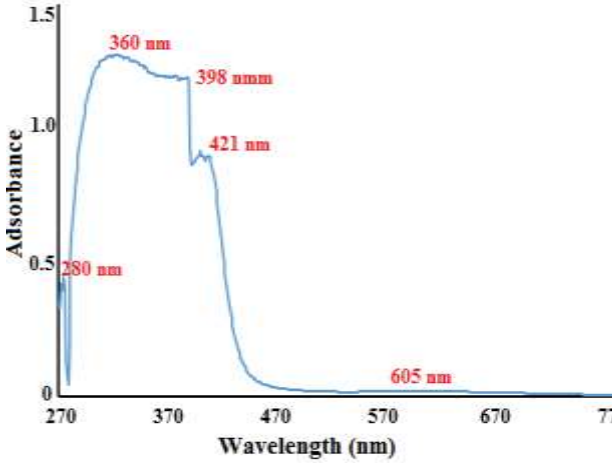

Figure. 8 Show the UV-Vis spectrum of copper complex (**2**) with a concentration of 10^{-5} mol/L in the DMSO.

3.4. Electrochemistry of the complexes (1and 2)

The electrochemical behavior of complex (**1**) and complex (**2**) was studied in a dimethyl sulfoxide solvent, shedding light on the redox process of the copper complexes (**Figs. (9, 10)**). The analysis of the voltammogram of the Cu (II) complex (**1**) showed distinctive reduction processes, including the reduction of Cu $^{(II)}$ to Cu $^{(I)}$ in the voltage range of -0.65 V, followed by the irreversible reduction of Cu $^{(I)}$ to Cu $^{(0)}$ in the range of -1.40 V [31, 43 ,45]. These observations show the redox activity of the Cu ions within the complex and provide insights into the electron transfer processes occurring during the reduction reactions. On the other hand, the voltammogram of the Cu (II) complex (**2**) exhibited a different electrochemical response, manifesting a cathodic voltammogram indicative of a quasi-reversible reduction process of Cu $^{(II)}$ to Cu $^{(I)}$ in the voltammogram range of -0.65 V. Furthermore, an anodic voltammogram was observed in the region of -0.47 V, attributed to the oxidation of Cu $^{(I)}$ to Cu $^{(II)}$ within the complex [31, 44, 45]. These findings highlight the redox behaviours of the copper cations within the complex (**2**) and suggest quasi- reversible redox processes occurring within the system.

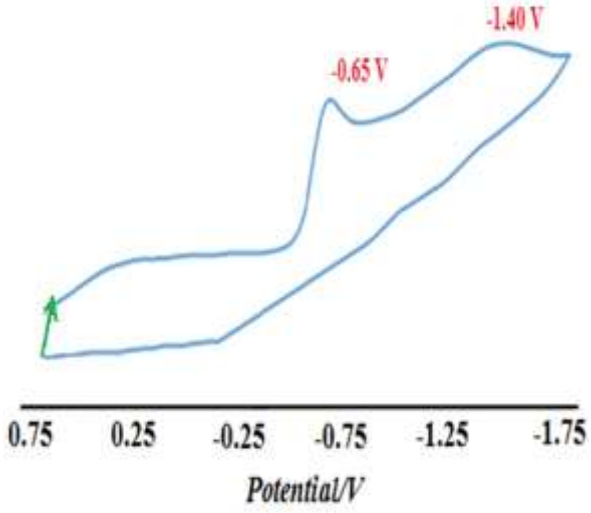

Figure. 9 Cyclic voltammogram of complex **(1)** inDMSO solutions.

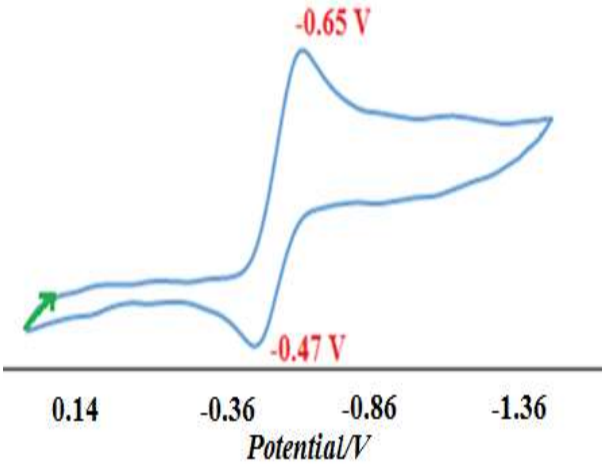

Figure. 10 Cyclic voltammogram of complex **(2)** inDMSO solutions.

3.5. Molecular docking

The inhibitory power of copper polymer complex (**1** and **2**) against the coronavirus (the two main proteins of this enzyme with the codes 6Y2F and

6M0J) has been investigated using the molecular docking method, so the best position of the studied compounds against the coronavirus is the receptors of the target proteins (6Y2F and 6M0J) with the most negative energy were selected and analysed. The total energy for complex (**1**) and (**2**) was -81.34 and -76.97 kcal/mol for 6Y2F protein and -118.98 and -135.68 kcal/mol for 6M0J protein, respectively. In this way, the copper polymer complex can be suggested as a suitable candidate to inhibit the coronavirus.

Molecular docking results showed that both complexes effectively interacted with the molecular targets of SARS-CoV-2 and penetrated the active site of the protein. Complex (**1**) is better than complex (**2**) with the lowest total energy (-81.34 kcal/mol) for 6Y2F protein targets and complex (**2**) is better than complex (**1**) with the lowest total energy (-135.68 kcal/mol) mol) for 6M0J protein targets performed better and more amino acids were able to penetrate into the active cavity and negative total energy was obtained. The molecular docking showed that complex (**1**) and complex (**2**) showed strong interactions with the target proteins of the coronavirus and successfully penetrated into the active sites of the proteins, forming various interactions such as van der Waals, carbon-hydrogen bonds, conventional hydrogen bond, and π-type interactions, etc. Therefore, these complexes can be recommended as suitable inhibitors for creating disorders. In **Table 1**, in order to better understand how the complexes, bind, the dominant interactions for the best inhibitors of each receptor are reported as non-covalent interactions with the surrounding amino acids. The complex (**1**) with the highest inhibitory activity against 6Y2F protein targets interacts with the following active amino acid residues, respectively:

LYS A:102, PHE A:103, VAL A:104, ARG A:105, ILE A:106, GLN A:110, ASN A:151, ILE A:152, ASP A:153, CYS A:156, SER A:158 **(Fig. 11).** As well as, complex (**2**) with the highest inhibitory activity against human ACE-2 target protein (6M0J) interacts with the following active amino acid residues, respectively:

PHE A:40, TRP A:69, THR A: 347, ALA A:348, TRP A:349, ASP A:350, LEU A:351, GLY A:352, PHE A:390, LEU A:391, 392, ARG A:393, ASN A:394, GLY A:395, HIS A: 401, LYS A:562 **(Fig. 12).**

The orientation of the copper complexes is almost similar so that the planar arrangement of the salicylaldehyde rings allows the complexes to stretch in the right direction in the active site of the receptors and interact well with amino acids. Planar amine rings are oriented towards the appropriate active site and bind to amino acids on the outer surface of the site. It should be noted that hydrophobic interactions of bromine atoms in complex (1) and interaction with polar parts of complex (2) have increased the inhibitory power of these complexes. Schiff base metal complexes can effectively increase the resistance through hydrophobic interaction. Fragments of the observed interactions, including hydrophobic interactions and coordination with the central metal, contribute to the stability and inhibitory activity of the complexes. These complexes show promising inhibitory effects through their interactions with the active sites of target proteins, paving the way for further research and development of new antiviral agents [44-48].

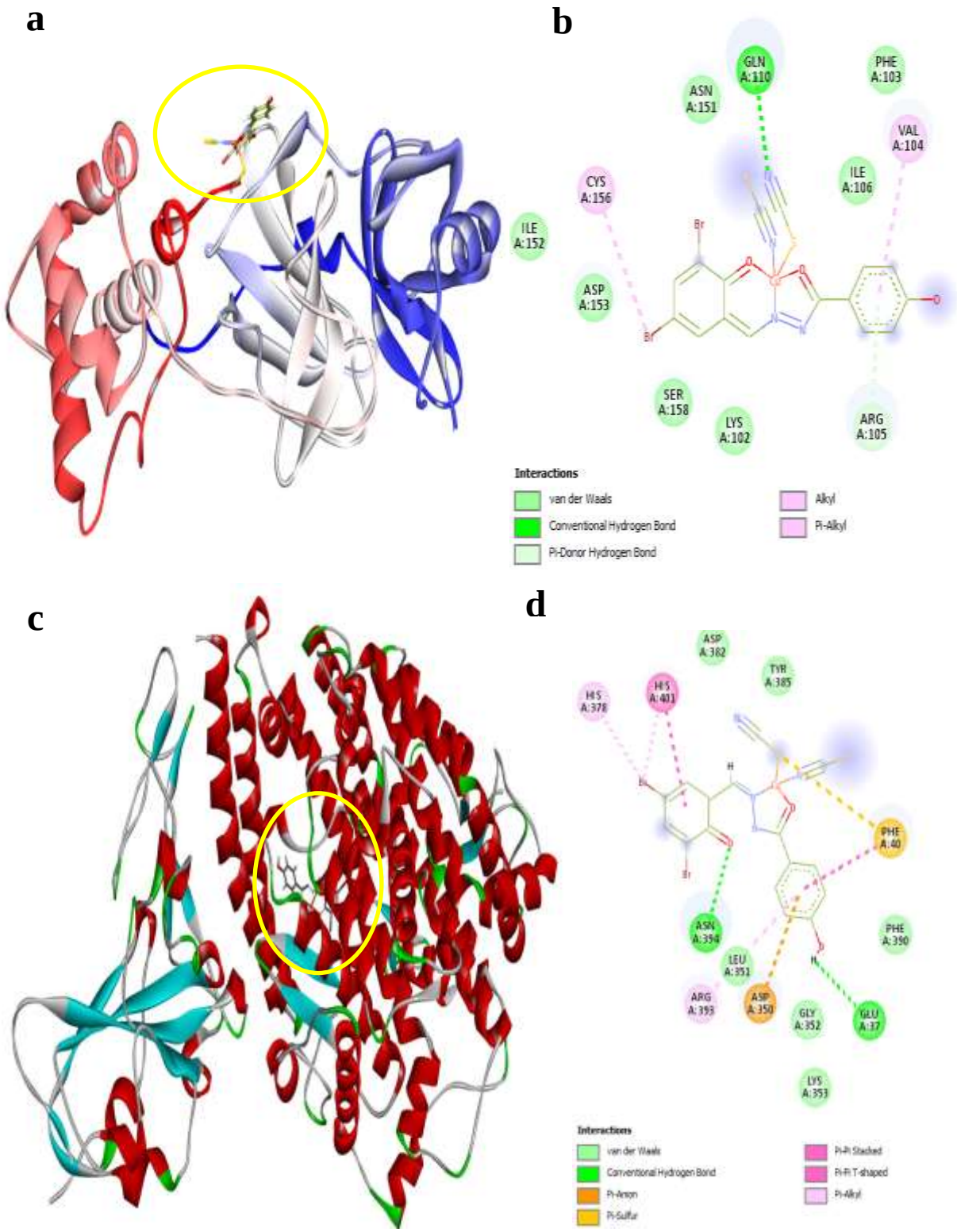

Figure. 11 (a, b) a, c docking model of the complex (**1**), b, d the binding method of the corresponding respective receptor inhibitor of the important amino acids involved (two and three-dimensional interactions) of (a, b: (ID: 6Y2F) and c, d: (ID: 6M0J)) complex (**1**), are shown.

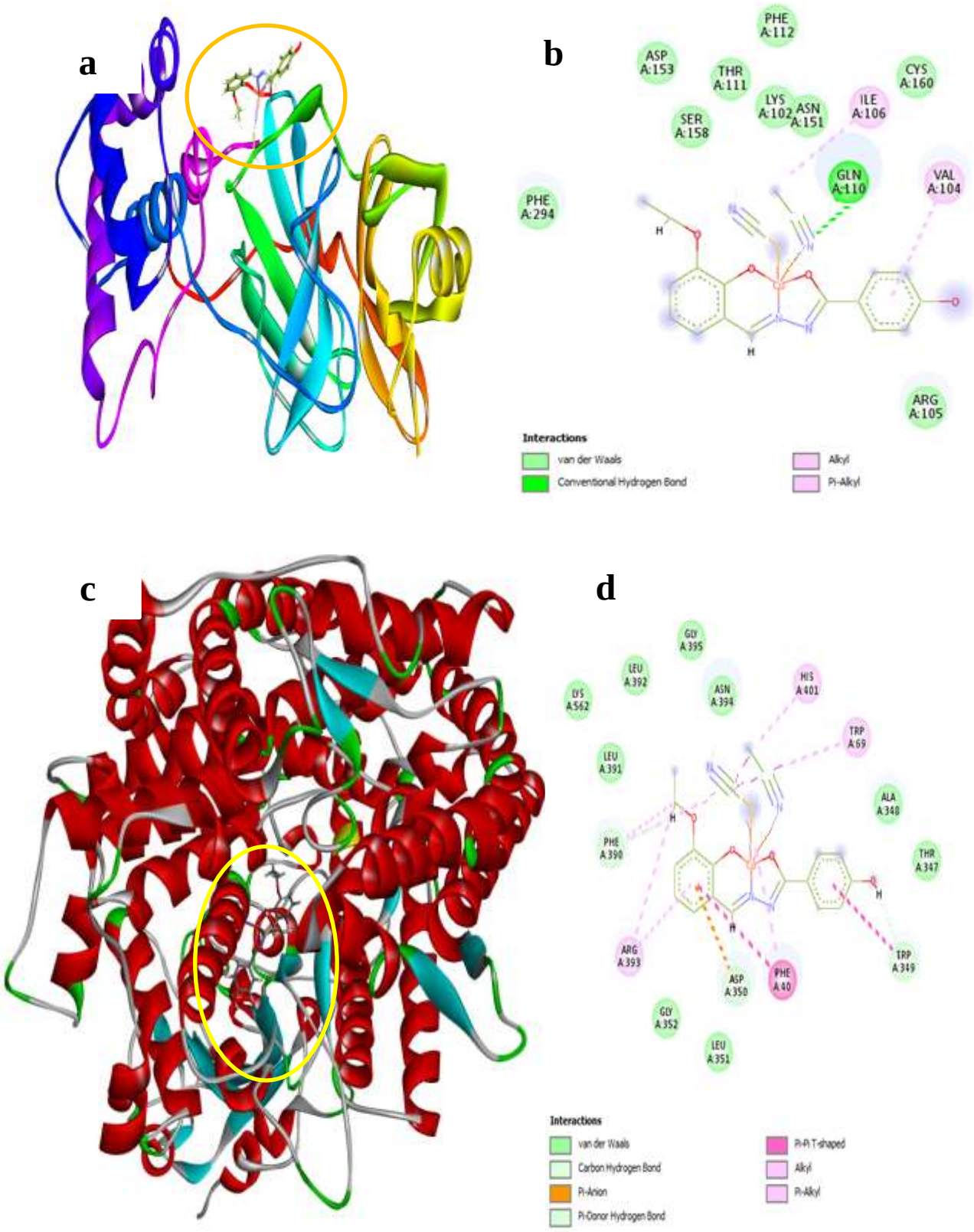

Figure. 12 (a, b) a, c docking model of the complex (**2**), b, d the binding method of the corresponding respective receptor inhibitor of the important amino acids involved (two and three-dimensional interactions) of (a, b: (ID: 6Y2F) and c, d: (ID: 6M0J)) complex (**2**), are shown.

Table. 1: The interaction of the amino acid of the active site of the receptor with the strongest inhibitor.

Complexes	Total energy of the system (kcal/mol)	Surrounding amino acids
Combined receptor: SARS-COV-2 protein (ID: 6Y2F)		
(1)	-81.34	LYS A:102, PHE A:103, VAL A: 104, ARG A:105, ILE A:106, GLN A:110, ASN A:151, ILE A:152, ASP A:153, CYS A:156, SER A:158.
(2)	-76.97	LYS A:102, VAL A: 104, ARG A:105, ILE A:106, GLN A:110, THR A:111, PHE A:112, ASN A:151, ASP A:153, SER A:158, CYS A:160, PHE A:294.
Combined receptor: human ACE-2 target protein (ID: 6M0J)		
(1)	-118.98	GLU A:37, PHE A:40, ASP A:350, LEU A:351, GLY A:352, LYS A:353, HIS A:378, ASP A:382, TYR A:385, PHE A:390, ARG A:393, ASN A:394, HIS A:401.
(2)	-135.68	PHE A:40, TRP A:69, THR A:347, ALA A:348, TRP A:349, ASP A:350, LEU A:351, GLY A:352, PHE A:390, LEU A:391, A:392, ARG A:393, ASN A:394, HIS A:401, LYS A:562

4 -Conclusion

Two copper polymer complexes derived from 4-hydroxybenzohydrazide and benzaldehyde were synthesized and characterized using various analytical techniques, including FT-IR, UV spectroscopy, elemental analysis, and cyclic voltammetry (CV). The identification of the complexes provided valuable insights into their chemical composition and structural properties, laying the foundation for further investigations. Then, the prepared polymer complexes were used as models to disrupt the function of two corona proteins using molecular docking simulation. By studying the ligand-protein interactions (ligand = studied compounds and protein = ٦Y2F and 6M0J for coronavirus), the total energies were calculated with values of about -81.34 kcal/mol (in the case of 6Y2F) and -135.68 kcal/mol (in the case of 6M0J). Based on the calculated total energy values, the copper polymer complexes derived from 4-hydroxybenzohydrazide and benzaldehyde are proposed as promising inhibitors against the targeted coronavirus proteins. The favorable total energy values indicate strong binding interactions between the compounds and the viral proteins, suggesting their potential efficacy as therapeutic agents or drug candidates for inhibiting the function of the coronaviruses under study. The calculated total energy values provide compelling evidence of the strong interactions between the compounds and experimental validation and in vitro studies can be pursued to validate the inhibitory activity of the copper polymer complexes and explore their therapeutic potential against the coronaviruses in question in the future.

Acknowledgments

We thank Semnan University for supporting this study. This research is supported by the Postdoc grant of the Semnan University (number 23336).

Institutional Review Board Statement

Not applicable.

Informed Consent Statement

Not applicable.

Conflicts of Interest

The authors declare no conflict of interest.

Appendixes

Appendixes appear after Conflicts of Interest.

Availability of data and materials

All data generated or analyzed during this study are included in this published article. Data available in article supplementary material, the data that supports the findings of this study are available in the supplementary material of this article.

Reference

[1] Yamada, S. (1966). Recent aspects of the stereochemistry of Schiff-base-metal complexes. *Coord. Chem. Rev.*, 1(4), 415-437.

[2] Rahman, L. H. A., Khatib, R. M. E., Nassr, L. A. E., Dief, A. M. A. Seleem, A. A. (2014). Design, Characterization, Teratogenicity Testing, Antibacterial, Antifungal and DNA Interaction of Few High Spin Fe (II) Schiff Base Amino Acid Complexes. *Spectrochim. Acta A*, 117, 366.

[3] Rahman, L. H. A., Khatib, R. M. E., Nassr, L. A. E., Dief, A. M. A., Seleem, A. A. (2014). Metal Based Pharmacologically Active Agents: Synthesis, Structural Characterization, Molecular Modeling, CT-DNA Binding Studies and In Vitro Antimicrobial Screening of Iron (II) Bromosalicylidene Amino Acid Chelates. *Spectrochim. Acta A*, 117, 366.

[4] Ran, X. G., Wang, L. Y., Lin, Y. C., Hao, Cao, J. D. R. (2010). Syntheses, characterization and biological studies of zinc(II), copper(II) and cobalt(II) complexes with Schiff base ligand derived from 2-hydroxy-1-naphthaldehyde and selenomethionine, *Appl. Organometal. Chem*., 24, 741.

[5] Shuai, Q., Chen, S., & Gao, S. (2007). Structural and thermal properties of three novel alkaline earth metal coordination polymers based on 5-hydroxyisophthalate ligand. *Inorganica Chim. Acta*, 360(5), 1381–1387.

[6] Bikas, R., Ghorbanloo, M., Sasani, R., Pantenburg, I., & Meyer, G. (2017). Manganese (II) complexes of hydrazone based NNO-donor ligands and their catalytic activity in the oxidation of olefins. *J. Coord. Chem*., 70(5), 819-830.

[7] Nikolova-Mladenova B.I., Momekov G.Ts. (2017). Synthesis, characterization and in vitro cytotoxic activity of zinc(II), cobalt(II) and nickel(II) complexes with tridentate ONO Schiff base 3-methoxysalicylaldehyde benzoylhydrazone, *Bulg Chem Comm, Special Edition B*, 49: 83-88.

[8] Deng, J., Gou, Y., Chen, W., Fu, X., & Deng, H. (2016). The Cu/ligand stoichiometry effect on the coordination behavior of aroyl hydrazone with copper (II): Structure, anticancer activity and anticancer mechanism. *Bioorg Med Chem*., 24(10), 2190-2198.

[9] Gomathi, G., & Gopalakrishnan, R. (2016). A hydrazone Schiff base single crystal (E)-Methyl N′-(3, 4, 5-trimethoxybenzylidene) hydrazine carboxylate: Physicochemical, in vitro investigation of antimicrobial activities and molecular docking with DNA gyrase protein. *Mater. Sci. Eng*., 64, 133-138.

[10] Harinath, Y., Reddy, D. H. K., Kumar, B. N., Apparao, C., & Seshaiah, K. (2013). Synthesis, spectral characterization and antioxidant activity studies of a bidentate Schiff base, 5-methyl thiophene-2-carboxaldehyde-carbohydrazone and its Cd (II), Cu (II), Ni (II) and Zn (II) complexes. *Spectrochim Acta A Mol Biomol Spectrosc*., 101, 264-272.

[11] Mahal, A., Abu-El-Halawa, R., Zabin, S. A., Ibrahim, M., Al-Refai, M., & Kaimari, T. (2015). Synthesis, characterization and antifungal activity of some metal complexes derived from quinoxaloylhydrazone. *World J. Org. Chem.*, 3(1), 1-8.

[12] Zubair, H., Azim, S., Ahmad, A., Khan, M. A., Patel, G. K., Singh, S., & Singh, A. P. (2017). Cancer chemoprevention by phytochemicals: Nature's healing touch. *Molecules*, 22(3), 395.

[13] Abdelgawad, M. A., Labib, M. B., & Abdel-Latif, M. (2017). Pyrazole-hydrazone derivatives as anti-inflammatory agents: Design, synthesis, biological evaluation, COX-1, 2/5-LOX inhibition and docking study. Bioorg Chem, 74, 212-220.

[14] Obasi, L. N., Kaior, G. U., Rhyman, L., Alswaidan, I. A., Fun, H. K., & Ramasami, P. (2016). Synthesis, characterization, antimicrobial screening and computational studies of 4-[3-(4-methoxy-phenyl)-allylideneamino]-1, 5-dimethyl-2-phenyl-1, 2-dihydro-pyrazol-3-one. *J. Mol. Struct.*, 1120, 180-186.

[15] Mondal, S., Pakhira, B., Blake, A. J., Drew, M. G. B., Chattopadhyay, Sh. K. (2016). Co(III) and Ni(II) complexes of an anthracene appended aroyl hydrazone: Synthesis, crystal structures, DNA binding and catecholase activity, *Polyhedron*, 117, 327-337.

[16] Qin, J., Zhao, S.S., Liu, Y.P., Man, Z.W., Wang, P., Wang, L.N., Xu, Y. and Zhu, H.L., (2016). Preparations, characterization, and biological features of mononuclear Cu (II) complexes based on hydrazone ligands. *Bioorg Med Chem Lett*, 26(20), 4925-4929.

[17] Xu, G., Tang, B., Gu, L., Zhou, P., & Li, H. (2016). Open coordination sites-induced structural diversity of a new series of Cu (II) complexes with tridentate aroylhydrazone Schiff base. *J. Mol. Struct*., 1120, 205-214.

[18] Meshram, U. P., Pethe, G. B., Yaul, A. R., Khobragade, B. G., & Narwade, M. L. (2017). Studies in stability constants of schiff base hydrazone complexes with transition metal ions. Effect of ligand on seed germination. *Russ. J. Phys. Chem. A*, 91, 1877-1882.

[19] Yousif, E. I., Ahmed, R. M., Hasan, H. A., Al-Fahdawi, A. S., & Al-Jeboori, M. J. (2017). Metal complexes of heterocyclic hydrazone Schiff-bases: preparation, spectral characterisation and biological study. *Iran. J. Sci. Technol. Trans. A: Sci.*, 41, 103-109.

[20] Begum, A.B., Rekha, N.D., Kumar, B.V., Ranganatha, V.L. and Khanum, S.A., (2014). Synthesis, characterization, biological and catalytic applications of transition metal complexes derived from Schiff base. *Bioorg. Med. Chem. Lett.*, 24(15), 3559-3564.

[21] Raman, N. and Mahalakshmi, R., (2014). Bio active mixed ligand complexes of Cu (II), Ni (II) and Zn (II): Synthesis, spectral, XRD, DNA binding and cleavage properties. *Inorg. Chem. Commun.*, 40, 157-163.

[22] Zhang, Y., Zhang, L., Liu, L., Guo, J., Wu, D., Xu, G., ... & Jia, D. (2010). Anticancer activity, structure, and theoretical calculation of N-(1-phenyl-3-methyl-4-propyl-pyrazolone-5)-salicylidene hydrazone and its copper (II) complex. *Inorganica Chim. Acta*, 363(2), 289-293.

[23] Deng, J., Chen, W., & Deng, H. (2016). Synthesis of dipyridyl ketone isonicotinoyl hydrazone copper (II) complex: structure, anticancer activity and anticancer mechanism. *J. Fluoresc.*, 26, 1987-1996.

[24] Shen, S., Chen, H., Zhu, T., Ma, X., Xu, J., Zhu, W., Chen, R., Xie, J., Ma, T., Jia, L. and

Wang, Y., (2017). Synthesis, characterization and anticancer activities of transition metal complexes with a nicotinohydrazone ligand. *Oncol. Lett.*, 13(5), 3169-3176.

[25] Du, Y., Chen, W., Fu, X., Deng, H., & Deng, J. (2016). Synthesis and biological evaluation of heterocyclic hydrazone transition metal complexes as potential anticancer agents. *RSC advances*, 6(111), 109718-109725.

[26] El-Behery, M. and El-Twigry, H. (2007) Synthesis, magnetic, spectral, and antimicrobial studies of Cu(II), Ni(II) Co(II), Fe(III), and UO_2(II) complexes of a new Schiff base hydrazone derived from 7-chloro-4-hydrazinoquinoline. *Spectrochimica Acta A*, 66, 28-36.

[27] Fekri, R., Salehi, M., Asadi, A., & Kubicki, M. (2017). DNA/BSA interaction, bio-activity, molecular docking simulation study and electrochemical properties of hydrazone Schiff base derived Cu (II)/Ni (II) metal complexes: Influence of the nuclearity and metal ions. *Polyhedron*, 128, 175-187.

[28] Martinez-Fleites,C., Smith, N.L., Turkenburg, J. P., Black, G. W., Taylor, E. J. (2009). Structures of two truncated phage-tail hyaluronate lyases from Streptococcus pyogenes serotype M1, *Acta Cryst*. F65, 963-966.

[29] Fekri, R., Salehi, M., Asadi, A., & Kubicki, M. (2018). Spectroscopic studies, structural characterization and electrochemical studies of two cobalt (III) complexes with tridentate hydrazone Schiff base ligands: Evaluation of antibacterial activities, DNA-binding, BSA interaction and molecular docking. *Appl. Organomet. Chem*., 32(2), e4019.

[30] You, Z.-L., & Zhu, H.-L. (2004). Bis(μ-2-amino pyridine) bis [(trifluoroacetato) silver (I)]. *Acta Crystallogr., Sect. C: Cryst. Struct. Commun.*, 60(10), m517–m519.

[31] Fekri, R., Salehi, M., Asadi, A., & Kubicki, M. (2019). Synthesis, characterization, anticancer and antibacterial evaluation of Schiff base ligands derived from hydrazone and their transition metal complexes. *Inorganica Chim. Acta*, 484, 245-254.

[32] Parvarinezhad, S., Salehi, M., Kubicki, M., & Eshaghi Malekshah, R. (2022). Experimental and theoretical studies of new Co (III) complexes of hydrazide derivatives proposed as multi‐target inhibitors of SARS‐CoV‐2. *Appl. Organomet. Chem*., 36(10), e6836.

[33] Wang, X.Y., Cao, G.B. and Yang, T. (2008). (E)-N′-(3, 5-Dibromo-2-hydroxy benzylidene) -4-hydroxy benzohydrazide monohydrate. *Acta Crystallogr. E: Structure Reports Online*., 64(10), o2022-o2022.

[34] Ayyannan, G., Veerasamy, P., Mohanraj, M., Raja, G., Manimaran, A., Velusamy, M., Bhuvanesh, N., Nandhakumar, R. and Jayabalakrishnan, C. (2017). Biological evaluation of organometallic palladium(II) complexes containing 4‐hydroxybenzoic acid (3‐ethoxy‐2‐hydroxy benzylidene) hydrazide: Synthesis, structure, DNA/protein binding, antioxidant activity and cytotoxicity. *Appl. Organomet. Chem*., 31(5), e3599.

[35] Ouennoughi, Y., Eddine Karce, H., Aggoun, D., Lanez, T., Ruiz-Rosas, R.,

Bouzerafa, B., Ourari, A., Morallon, E., (2017). A novel ferrocenic copper(II) complex Salen-like, derived from 5-chloromethyl-2-hydroxyacetophenone and N ferrocenmethylaniline: Design, spectral approach and solvent effect towards electrochemical behavior of Fc+/Fc redox couple, J. Organ. Chem., 848, 344-351.

[36] Deilami, A.B., Salehi, M., Arab, A. & Amiri, A., (2018). Synthesis, crystal structure, electrochemical properties and DFT calculations of three new Zn(II), Ni(II) and Co(III) complexes based on 5-bromo-2-((allylimino)methyl) phenol Schiff-based ligand. Inorganica Chim. Acta, 476, 93-100.

[37] Gholivand, K., Barzegari, A., Yousefian, M., Malekshah, R.E., & Faraghi, M., (2023). Experimental and theoretical evaluation of biological properties of a phosphoramide functionalized graphene oxide *Biocatal. Agric. Biotechnol*, 47, 102612.

[38] Gholivand, K., Sabaghian, M., & Malekshah, R. E., (2021). Synthesis, characterization, cytotoxicity studies, theoretical approach of adsorptive removal and molecular calculations of four new phosphoramide derivatives and related graphene oxide. *Bioorg. Chem.*, 115, 105193.

[39] Ramezanipoor, S., Parvarinezhad, S., Salehi, M., Grześkiewicz, A. M., & Kubicki, M., (2022). Crystal structures, electrochemical properties and theoretical studies of three New Zn(II), Mn(III) and Co(III) Schiff base complexes derived from 2-hydroxy-1-allyliminomethyl-naphthalen. *J. Mol. Struct.*, 1257, 132541.

[40] Sepehrfar, S., Salehi, M., Parvarinezhad, S., Grześkiewicz, A.M., & Kubicki, M., (2023). New Cu(II), Mn(II) and Mn(III) Schiff base complexes cause noncovalent interactions: X-ray crystallography survey, Hirshfeld surface analysis and molecular simulation investigation against SARS-CoV-2. *J. Mol. Struct.*, 1278, 134857.

[41] Arjun, H.A., Rajan, R.K., Elancheran, R., Ramanathan, M., Bhattacharjee, A. and Kabilan, S. (2020). Crystal structure, Hirshfeld surface analysis, DFT and molecular docking studies on benzohydrazide derivatives as potential inhibitors of prostate cancer. *Chem. Data Collect*., 26, 100350.

[42] Kanmazalp, S.D., Dege, N., Ilhan, I.O. and Akin, N. (2020). Crystal Structure and Hirshfeld Surface Analysis of 3, 5-Bis (4-Methoxyphenyl)-4, 5-Dihydro-1 H-Pyrazole-1-Carbothioamide. *J. Struct. Chem*., 61(1), 126-132.

[43] Akkurt, M., Duruskari, G.S., Toze, F.A., Khalilov, A.N. and Huseynova, A.T. (2018). Crystal structure and Hirshfeld surface analysis of (E)-3-[(2, 3-dichlorobenzylidene) amino]-5-phenylthiazolidin-2-iminium bromide. Acta Crystallogr. E: Crystallogr. Commun., 74(8), 1168-1172.

[44] Parvarinezhad, S., Salehi, Kubicki, M., & Eshaghi Malekshah, R., (2022). Synthesis, characterization, spectral studies and evaluation of noncovalent interactions in co-crystal of μ-oxobridged polymeric copper(II) complex derived from pyrazolone by theoretical studies. *J. Mol. Struct.*, 1260,132780.

[45] Parvarinezhad, S., Salehi, M., Eshaghi Malekshah, R., Kubicki, M., & Khaleghian, A., (2022). Synthesis, characterization, spectral studies two new transition metal complexes derived from pyrazolone by theoretical studies, and investigate anti-proliferative activity. *Appl. Organomet. Chem*., 36(3), e6563.

[46] Ghasemi, L., Behzad, M., Gharib, A., Arab, A., & Abbasi, A., (2023). A pyrazolone-based dinuclear Cu(II) Schiff-base complex: DFT studies on the rate-determining steps of the tautomerism in the ligand and molecular docking modelling with COVID-19 main protease (6LU7). *J. Coord. Chem*., 76(5-6), 830-846.

[47] Parvarinezhad, S., Salehi, M., Kubicki, M., & Khaleghian A., (2021). Unprecedented formation of a μ-oxobridged dimeric copper (II) complex: Evaluation of structural, spectroscopic, and electronic properties by using theoretical studies and investigations biological activity studies of new Schiff bases derived from pyrazolone. *Appl. Organomet. Chem*., 35(12), e6443.

[48] Ghasemi, L., Abedi, A., Abbasi, A., Kucerakova, M., Dusek, M., Behzad, M. (2024). Subtle structural variations in new mixed-ligand Cu(II) complexes with NN'O type unsymmetrical Schiff bases: Molecular docking against SARS-Cov-2 and its Omicron variant main proteases, *Inorg. Chem. Commun*.159, 111795.